THE JOURNAL OF BIOLOGICAL CHEMISTRY
Vol. 280, No. 28, Issue of July 15, pp. 26526–26532, 2005

Three Distinct Molecular Surfaces in Ephrin-A5 Are Essential for a Functional Interaction with EphA3*[S]

Received for publication, May 5, 2005
Published, JBC Papers in Press, May 18, 2005, DOI 10.1074/jbc.M504972200

Bryan Day‡§, Catherine To§¶, Juha-Pekka Himanen§‖, Fiona M. Smith‡, Dimitar B. Nikolov‖, Andrew W. Boyd‡, and Martin Lackmann¶‡‡**

*From the ‡Queensland Institute of Medical Research, P. O. Royal Brisbane Hospital 4029, Queensland, Australia, ¶Department of Biochemistry and Molecular Biology, Monash University, Clayton, Melbourne, Victoria 3168, Australia, ‖Structural Biology Program, Memorial Sloan-Kettering Cancer Center, New York, New York 10021, and **Department of Medicine, University of Queensland, P. O. Royal Brisbane Hospital 4029, Queensland, Australia*

Eph receptor tyrosine kinases (Ephs) function as molecular relays that interact with cell surface-bound ephrin ligands to direct the position of migrating cells. Structural studies revealed that, through two distinct contact surfaces on opposite sites of each protein, Eph and ephrin binding domains assemble into symmetric, circular heterotetramers. However, Eph signal initiation requires the assembly of higher order oligomers, suggesting additional points of contact. By screening a random library of EphA3 binding-compromised ephrin-A5 mutants, we have now determined ephrin-A5 residues that are essential for the assembly of high affinity EphA3 signaling complexes. In addition to the two interfaces predicted from the crystal structure of the homologous EphB2·ephrin-B2 complex, we identified a cluster of 10 residues on the ephrin-A5 E α-helix, the E–F loop, the underlying H β-strand, as well as the nearby B–C loop, which define a distinct third surface required for oligomerization and activation of EphA3 signaling. Together with a corresponding third surface region identified recently outside of the minimal ephrin binding domain of EphA3, our findings provide experimental evidence for the essential contribution of three distinct protein-interaction interfaces to assemble functional EphA3 signaling complexes.

Signaling by Eph receptors (Ephs)[1] and their cell surface-associated ephrin ligands forms an essential part of a highly conserved molecular mechanism coordinating cell migration and positioning during normal and oncogenic tissue development (1). In general, the path of Eph-expressing cells or axons is directed through contact-dependent cell-cell adhesion or repulsion (2), whereby competing interactions of neighboring Eph-expressing cells for ephrin targets govern the final cell position as the biological outcome (3). Many biological effects attributed to Eph function require concurrent "forward" signaling in Eph-expressing cells and "reverse" signaling in ephrin-expressing cells (4, 5). In contrast to the prototypical activation mechanism of receptor tyrosine kinases, Eph signaling is activated by the assembly of ephrin/Eph oligomers into large clusters. Ephs are composed of conserved structural modules. They include a unique N-terminal ephrin binding domain (6–8) forming a globular β-barrel (9), a cysteine-rich linker and epidermal growth factor-like region, and two fibronectin type III repeats. The cytoplasmic part contains an uninterrupted, tyrosine kinase domain (10) and several protein-protein interaction modules, including Src homology 2-docking sites, a sterile-α-motif, and a C-terminal PDZ binding motif (11). Structural features broadly classify six glycophosphatidyl inositol membrane-anchored ephrins as A-type, which "promiscuously" can bind and activate nine type-A Ephs, as well as three transmembrane ephrins as B-type, which contain conserved cytoplasmic domains and activate six type-B Ephs (12). It is now clear that this grouping is likely an oversimplification, and in particular, EphA4 and EphB2 bind and become activated by both A- and B-type ephrins (13, 14). This characteristic promiscuity of functionally relevant Eph/ephrin interactions is possibly because of the high structural conservation of Eph and ephrin binding domains. Crystal structures of the interacting domains of EphB2, ephrin-B2, and ephrin-A5 and of their complexes (8, 9, 14, 15) revealed that the initial 1:1 Eph/ephrin contacts (16) are provided by a deep Eph surface channel formed by β-strands (D, E, G, J, M), which buries the extended, hydrophobic ephrin G–H loop (8). In the crystal structure of the EphB2·ephrin-B2 complex, a second lower affinity heterotetramerization interface facilitates formation of a 2:2 cyclic complex comprising two Eph/ephrin heterodimers (see Fig. 3). Although comparatively small, the tetramerization interface is critical for the assembly of stable, signaling-competent Eph clusters (17), and in agreement with its postulated role of providing subclass binding specificities (8), is not present in the structure of the EphB2·ephrin-A5 complex (14).

Although there is little doubt that the Eph/ephrin heterotetramers are the essential building block of Eph signaling complexes, downstream signaling requires the assembly of higher order oligomers (18). *In vitro*, this is routinely achieved through Eph activation by preclustered, tetravalent ephrin-Fc fusion proteins (19). The available crystal structures leave unclear how Ephs and ephrins assemble into the oligomeric signaling

* This work was supported by grants from the National Health and Medical Research Council of Australia (284428, 234707) (to M. L. and A. W. B.) and National Institutes of Health Grant RO1-NS38486 (to D. B. N.). The costs of publication of this article were defrayed in part by the payment of page charges. This article must therefore be hereby marked "*advertisement*" in accordance with 18 U.S.C. Section 1734 solely to indicate this fact.

[S] The on-line version of this article (available at http://www.jbc.org) contains supplemental Table 1.

The atomic coordinates and structure factors (code 1SHX) have been deposited in the Protein Data Bank, Research Collaboratory for Structural Bioinformatics, Rutgers University, New Brunswick, NJ (http://www.rcsb.org/).

§ These authors made equal contributions to this work and are thus regarded as joint first authors.

‡‡ To whom correspondence should be addressed: Dept. of Biochemistry and Molecular Biology, P.O. Box 13D, Monash University, Victoria 3800, Australia. Tel.: 613-9905-3738; Fax: 613-9905-3726; E-mail: martin.lackmann@med.monash.edu.au.

[1] The abbreviations used are: Ephs, Eph receptors; TEV, tobacco etch virus; HEK, human embryonic kidney; w/t, wild-type; IP, immunoprecipitation.

complexes that are required for biological responses (11, 18) and suggest the involvement of Eph/ephrin contact regions outside the crystallized domains. Indeed, earlier studies indicated the presence of ephrin-independent Eph/Eph contacts located C-terminally of the globular domain that are important for EphA3 function (7). Furthermore, a recent analysis of ephrin-A5 binding-compromised EphA3 mutants revealed, in addition to the two structurally defined ephrin binding sites, a third functional binding interface outside the crystallized domain (17). This site, although contributing only modestly to ligand binding, is essential for receptor phosphorylation, recruitment of signaling molecules, and downstream responses, supporting the notion that the tetrameric Eph·ephrin complex observed in the crystal structure is necessary (but not sufficient) for signaling. The position of the newly identified binding site within the cysteine-rich linker that connects the ephrin binding and Eph-Eph dimerization domains suggests that ephrin binding may cause a reorientation of Ephs that facilitates their assembly into oligomeric clusters (17).

We have now applied the same random mutagenesis approach previously used to identify ephrin-A5-interacting residues in EphA3 to assign the molecular determinants of ephrin-A5 that mediate EphA3 binding. In this case, the recently elucidated crystal structure of ephrin-A5 in complex with EphB2 (14) allowed the selection, structural alignment, and functional analysis of EphA3 binding-compromised ephrin-A5 mutants from a library of random point mutants spanning the whole N-terminal receptor binding domain of ephrins. Our analysis revealed a number of critical residues that confirm the two Eph binding sites shown in the crystal structure of the of the EphB2·ephrin-B2 complex (8). We also uncover a potential third Eph-interacting surface, the existence of which had been implied by the EphA3 mutagenesis study (17). This new site, which likely mediates Eph/ephrin clustering interactions, includes the protruding ephrin-A5 E α-helix and E–F loop, the underlying H β-strand, as well as the nearby B–C loop. Its location, between the dimerization and tetramerization sites, is consistent with a corresponding interaction surface on EphA3 that is closely adjacent to the Eph globular domain. Kinetic and functional analysis of representative mutants confirms the notion that engagement of each of the three identified Eph binding sites of ephrin-A5 is required to elicit cell-morphological responses in EphA3-expressing cells.

MATERIALS AND METHODS

Reagents

The anti-EphA3 monoclonal antibody, IIIA4, and the affinity-purified rabbit polyclonal antibodies were previously described (16, 20). Other antibodies and reagents were from Transduction Laboratories (anti-CrkII), Upstate Biotechnology (4G10), New England Biolabs (P-Tyr100), Jackson Laboratories (horseradish peroxidase-conjugated anti-mouse antibodies), and Bio-Rad (horseradish peroxidase-conjugated anti-rabbit).

Protein Expression and Purification

EphA3 and Ephrin-A5-Fc Fusion Proteins—Recombinant protein containing the EphA3 extracellular domain fused to the human IgG1 hinge and Fc regions (EphA3-Fc) was prepared as described previously (17). For the expression of ephrin-A5-Fc, we prepared a cDNA encoding ephrin-A5 (GenBank™ accession number NM_001962) residues Met^{1}–Ala^{204}, followed by the consensus sequence ENLYFQG corresponding to the protease cleavage site of the tobacco etch virus (TEV) protease, followed by the IgG1 hinge and Fc regions of human IgG1. The product was cloned in-frame into the unique BamHI site of the pIgBOS vector. EphA3-Fc and ephrin-A5/TEV-Fc DNA were stably transfected into Chinese hamster ovary cells, and the proteins were purified from immunoglobulin-depleted cell culture supernatants on protein-A-Sepharose and ion exchange MonoQ columns under conditions described previously (22). For large scale protein production, ephrin-A5-Fc-expressing cells were grown in IgG-free culture medium using cellulose acetate hollow fiber bioreactors (Cellex Biosciences, Minneapolis, MN) as described previously (14).

TABLE I
Summary of the random mutagenesis screen

Yeast colonies transfected with YEpFLAG-1 encoding mutant, soluble ephrin-A5 proteins were selected by probing three consecutive nitrocellulose filters containing absorbed proteins from individual yeast colonies with anti-FLAG and anti-Myc antibodies, EphA3-Fc, and with appropriate secondary antibodies. Only clones secreting ephrins with N- and C-terminal FLAG and Myc epitopes, respectively, were further considered. Approximately similar numbers of colonies secreting EphA3-binding (+) or -binding-compromised (−) mutant ephrins were analyzed. As some clones express ephrin-A5 proteins with more than one mutation (see "Materials and Methods"), the number of mutations is > the number of colonies.

FLAG/Myc epitope present	EphA3 binding	No. of mutations analyzed	% of total analyzed mutations	No. of colonies	% of total colonies analyzed
+	−	77	48.5	40	48
+	+	82	51.5	44	52

Yeast Ephrin-A5 Expression—The ephrin-A5 fragment (Gln^{21}–Ser^{199}) was generated by PCR from the wild-type ephrin-A5 cDNA (GenBank™ accession number NM_001962) in pBluescript using primers corresponding to nucleotides 344–362 and 862–879 and cloned into a modified (17) YEpFLAG-1 (Sigma) yeast expression vector. This expression vector positions the ephrin coding sequence between N- and C-terminal FLAG and Myc epitopes, respectively, allowing detection of the full-length protein with anti-FLAG antibody (M2, Sigma) and/or the anti-Myc antibody (9E10, a generous gift from Dr. D. Huang, Walter and Eliza Hall Institute, Melbourne, Australia).

Random Mutagenesis

Random point mutants of the ephrin-A5 extracellular domain were created using non-stringent PCR (17, 23). Conditions were optimized to yield 3–4 mutations or 1–3 amino acid changes/clone, so that 500 independent clones with some 1000 mutated amino acid residues provided a four-fold mutational coverage of the target sequence. A library of random point mutants was initially prepared in *Escherichia coli*. The plasmid cDNAs from pooled colonies (~17,000) were then transfected into the *Saccharomyces cerevisiae* strain BJ3505, and yeast colonies expressing mutant ephrin-A5 proteins were screened with monoclonal antibodies against the Myc (9E10) and FLAG (M2) epitopes and with EphA3-Fc as described previously (17). Individual filters from each set of replicates were probed with horseradish peroxidase-conjugated anti-mouse and anti-human IgG antibodies (Dako). Colonies showing reduced EphA3-Fc binding were recovered and DNA extracted for sequence analysis of the ephrin-A5 (XhoI-BglII) inserts.

Site-directed Mutagenesis and Transient Protein Expression

To determine relevant mutations in critical ephrin-A5 clones containing >1 amino acid change, individual mutations were introduced into the ephrin-A5/TEV-Fc mammalian expression vector by site-directed mutagenesis (QuikChange mutagenesis kit, Stratagene). Following transient transfection into HEK293T cells (FuGENE 6, Roche Applied Sciences), mutant and wild-type (w/t) ephrin-A5/TEV-Fc proteins were purified from culture supernatants using protein-A and ion exchange chromatography as described under "EphA3 and Ephrin-A5-Fc Fusion Proteins." Protein expression was assessed by Western blot (anti-human IgG horseradish peroxidase) and by BIAcore analysis using sensor chips with parallel surfaces containing immobilized EphA3, anti-human IgG antibody, and single chain ephrin-A5.

Surface Plasmon Resonance Analysis

Analysis of protein interactions by surface plasmon resonance was carried out on a BIAcore 2000 biosensor (BIAcore) as described previously (17). Purified wild-type and mutant ephrin-A5 extracellular domain proteins were analyzed on parallel EphA3-Fc- and ephrin-A5-derivatized CM5 sensor chips (BIAcore 2000 optical biosensor, BIAcore AB, Sweden). The concentrations of high pressure liquid chromatography-purified proteins were determined from absorbance measurements at 215 nm. Samples of purified ephrin-A5 extracellular domain (62.5–1000 ng/ml) were analyzed in each assay. Interaction kinetics were evaluated from seven serial dilutions of each sample by Global Analysis using the BIAevaluation software (version 3.1).

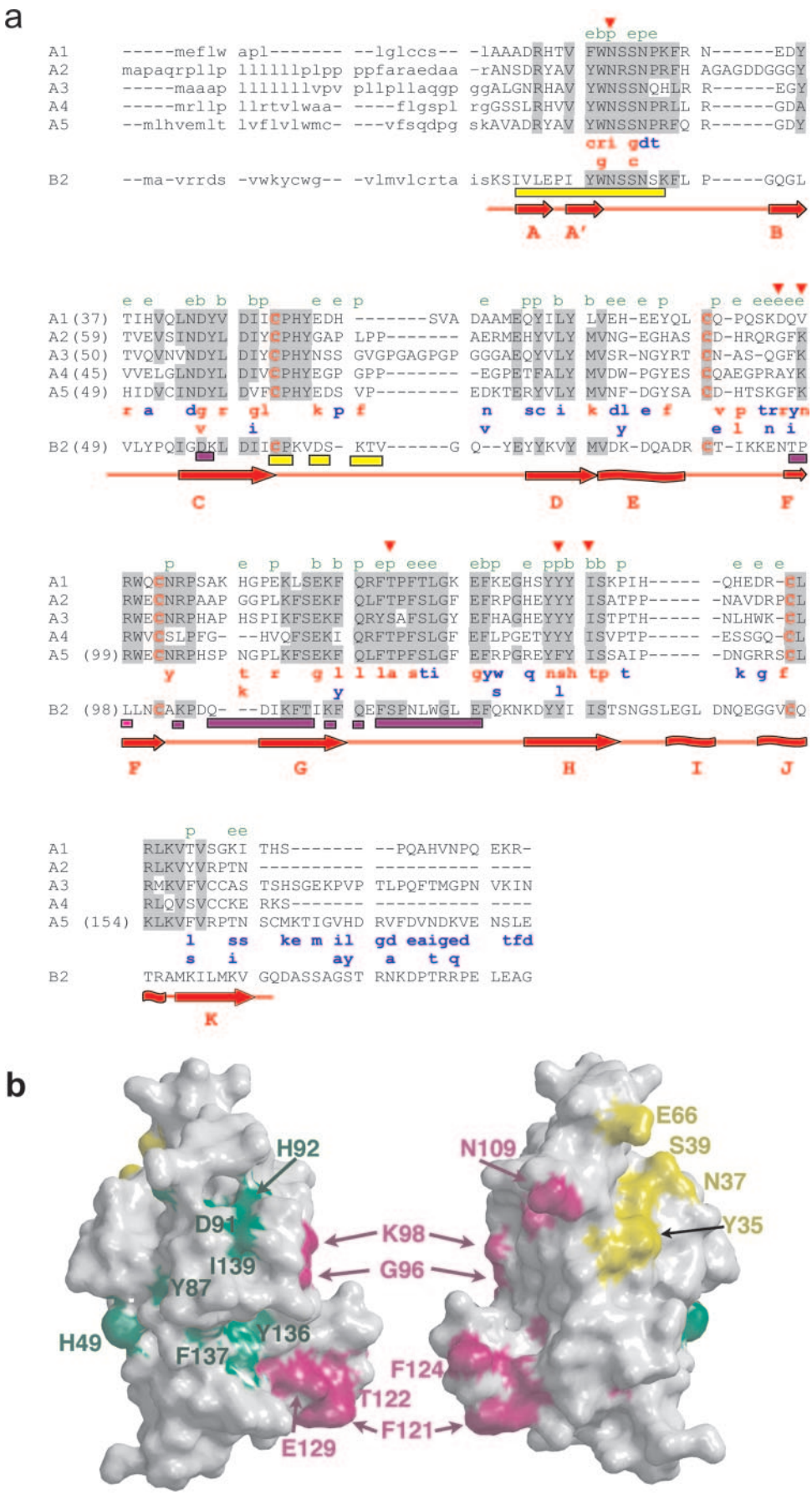

FIG. 1. **Location of ephrin-A5 point mutants within the amino acid sequences of human A-type ephrins and ephrin-B2.** *a*, the alignment gaps were adopted from a ClustalX (1.81) multiple sequence alignment of all known ephrin sequences, excluding *Drosophila* ephrin. Residues that are conserved in four or more ephrins are *shaded gray*. Ephrin-A5 point mutants not affecting binding and mutants that compromise

Cell Manipulations, Immunoprecipitation, Western Blotting, and Microscopy

The HEK293 cells that were stably transfected with full-length EphA3 have been described previously (24, 25). Following stimulation of these cells for 10 min with 1.5 μg/ml preclustered, w/t, or mutant ephrin-A5-Fc, Triton X-100 cell lysates were prepared, and even portions (50% v/v) were subjected to immunoprecipitation (IP) with anti-EphA3 monoclonal antibody IIIA4 affinity beads or anti-CrkII monoclonal antibody/protein-A-Sepharose as described previously (24). The anti-CrkII IPs and ⅓ of the anti-EphA3 IPs were probed with anti-EphA3 and anti-phosphotyrosine antibodies, respectively. To assess even gel loading, 8% (v/v) of each anti-EphA3 IP was probed with anti-EphA3 antibodies.

RESULTS

Expression Library Screen for EphA3 Binding-defective Ephrin-A5 Mutants—To define critical Eph binding and signal initiation residues in ephrin-A5, we subjected most of the extracellular domain (residues Gln^{21}–Ser^{199}) to random mutagenesis, excluding only the N-terminal signal sequence and C-terminal unstructured residues. The experimental conditions, previously optimized to assign critical EphA3 surfaces (17), resulted in a four-fold mutational coverage of the ephrin-A5 sequence. This corresponds to a library of some 1000 mutants, which are randomly distributed across the entire target sequence. Only mutations that had generated full-length secreted proteins containing both the N-terminal FLAG and the C-terminal Myc tags (assayed with anti-FLAG and anti-antibodies) were selected for further analysis (Table I). A total of 84 colonies with an average of two amino acid substitutions were sequenced. The ephrin-A5 proteins secreted from these colonies were further assayed for binding of EphA3-Fc, revealing that 44 clones produced ephrins that retained EphA3 binding capacity, whereas 40 mutants had lost this capacity.

The EphA3 Binding Mutants Define Three Distinct Contact Surfaces—For an initial assessment of their functional relevance, we mapped these mutations onto the wild-type sequences of human A-type ephrins, as well as ephrin-B2 (Fig. 1*a*), all of which bind with varying affinities to EphA3 (16, 26). A total of 33 amino acid substitutions that affect the EphA3 binding map to the crystallized portion of ephrin-A5, whereby most (21/33) of the corresponding residues are conserved in five or all of the six aligned ephrins. Some 19 of these 21 mutations are located within (or immediately adjacent to) the proposed heterodimerization (12/33) or heterotetramerization (7/33) molecular surfaces. Importantly, a cluster of 5 mutations that compromised EphA3 binding was found within the highly conserved sequence motif YY(F)Y(I)IS on the "H" α-strand. This strand packs against the protruding E α-helix and the long E–F loop that harbor 4 additional mutations. Together with the nearby B–C loop, containing one mutation, these secondary structure elements generate an ephrin surface positioned between the dimerization and tetramerization interfaces (Fig. 1*b*; see also Fig. 3), which is not in direct Eph contact in the Eph-B2/ephrin-B2 structure, (14). The clustered localization of these residues suggests that they define a distinct third interaction site of the EphA3·ephrin-A5 complex.

For comparison, we also mapped the 44 amino acid substitutions that did not alter the binding to EphA3. Only 9 of the 44 affected conserved residues (in at least four of the aligned ephrins), and 7 of these were conservative substitutions (Asp → Asn, Ser → Thr, Leu → Ile, or Phe → Tyr). Notably, mutations in 16 (of the 24) juxtamembrane ephrin-A5 residues did not affect EphA3 binding, confirming that this unstructured region is not involved in Eph/ephrin interactions.

Kinetic Analysis of Selected Ephrin-A5 Mutants—The mapping of the amino acid substitutions onto the ephrin-A5 structure in the context of known Eph/ephrin contacts allowed us to select six mutants for functional analysis, including representatives for each of the previously defined interfaces. We introduced these mutations into an expression vector encoding ephrin-A5 fused to the Fc part of human IgG and separated by an engineered TEV protease cleavage site, allowing production of monomeric ephrin-A5 as well as dimeric Fc-fusion derivatives from the same expression construct. For surface plasmon resonance analysis, monomeric ephrins were released by TEV cleavage (Fig. 2*a*, *inset*), and their binding to the EphA3 ectodomain or bovine serum albumin as non-relevant control proteins was tested on parallel BIAcore sensor surfaces (Fig. 2*a*).

The kinetic analysis of the ephrin-A5 mutants revealed that a substitution of the G–H loop residue Thr^{122} with an alanine profoundly reduces the association rate and increases the dissociation rate of the EphA3/ephrin-A5 interaction (Table II), resulting in marginal micromolar affinity binding (Fig. 2*a*). This observation confirms previous findings, indicating that the major contribution to the binding affinity is provided by docking of the ephrin G–H loop into the ligand binding Eph channel at the heterodimerization interface (8, 17). By comparison, amino acid substitutions on the ephrin "D" β-strand (Gly^{96} → Arg and Lys^{98} → Asn), which binds along the upper convex surface of the receptor at the Eph/ephrin dimerization interface, affect EphA3/ephrin-A5 interaction less dramatically, yielding only a 3–4-fold decrease in the binding affinity (41 and 60 nM, respectively).

Not surprisingly, a similarly pronounced effect upon EphA3 recognition and binding was observed for the mutation Asn^{37} → Ile, located at the base of the ephrin A–B loop at the tetramerization interface. Its almost 10-fold affinity drop from 13 to 122 nM was primarily the result of a substantially reduced association rate of the mutant protein (2.8×10^4 M s^{-1}) compared with w/t ephrin-A5 (1.1×10^6 M s^{-1}, Table II).

Importantly, two of the point mutations, Phe^{137} → Ser and Ile^{139} → Thr, located between the previously characterized dimerization and tetramerization surfaces (see Fig. 1*b*), affect EphA3 binding to an extent comparable with that of the dimerization interface mutations Gly^{96} → Arg and Lys^{98} → Asn. Specifically, the mutated residues map to the conserved H-strand, where they mediate its packing against the "E" helix at the ephrin-A5 molecular surface. Phe^{137} and Ile^{139} are far from the dimerization (~20 Å of distance to the tip of the G–H loop) and tetramerization interfaces, and it is doubtful their mutation would affect the structure of these ephrin binding sites. More likely, they would only affect the local molecular surface and, in particular, the positioning and/or conformation of the protruding E–F loop and E helix relative to the underlying β-barrel scaffold. We postulate that this surface region, to-

binding to EphA3 (maximally two mutations/residue shown) are indicated *under* the ephrin-A5 sequence in *blue* and *red bold lowercase letters*, respectively. *Red triangles above* the sequences indicate point mutants that were subjected to detailed functional analysis. The N-terminal sequences, not present in the crystal structures of ephrin-B2 (8) and ephrin-A5 (14), are given in *lowercase lettering*. Secondary structure elements according to the ephrin-B2 and ephrin-A5 crystal structures are illustrated as *arrows* for β-sheets and *waved rectangles* for helices. *Purple* and *yellow boxes underlining* the ephrin-B2 sequence indicate residues in the dimerization and tetramerization interfaces, respectively. *Above* the alignment, in *green letters*, is indicated whether the residues are surface exposed (*e*), buried (*b*), or partially buried (*p*). A list of the surface-exposed areas of all ephrin-A5 residues is provided as supplemental Table 1. *b*, molecular surface of ephrin-A5 (Protein Data Bank code 1SHX) *highlighting* all residues identified in this study that harbor Eph binding-defective mutations. The mutated residues in the previously characterized heterodimerization interface are in *magenta*, the mutated residues in the heterotetramerization interface are in *yellow*, and all other mutated residues are in *green*.

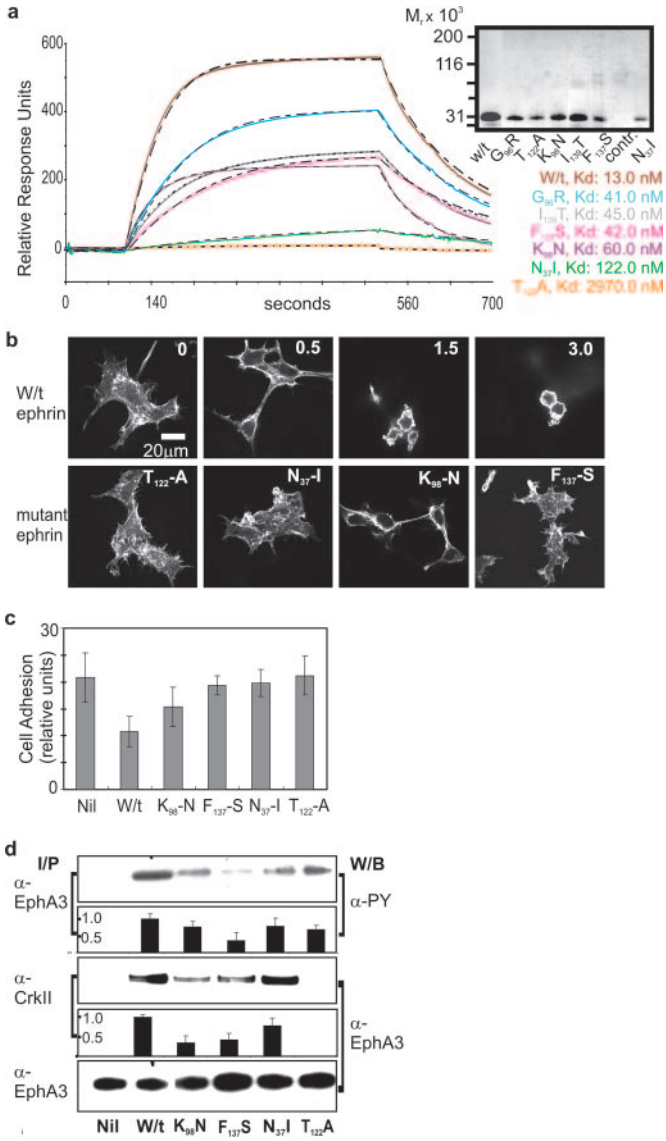

FIG. 2. **Functional analysis of selected EphA3 binding-compromised ephrin-A5 mutants.** Ephrin-A5-Fc fusion proteins (w/t or containing indicated amino acid substitutions) were purified on protein-A-Sepharose from supernatants of transiently expressed HEK293 cells and subjected to kinetic analysis by surface plasmon resonance (*a*), or to cell-based functional analysis (*b–d*). *a*, for BIAcore assays, TEV-cleaved proteins were purified by ion exchange high pressure liquid chromatography and analyzed by SDS-PAGE/silver staining (*inset*) prior to analysis on a sensor chip containing the EphA3 exodomain. BIAcore sensorgrams illustrate binding of ephrin-A5 (w/t or mutant as indicated) at the maximal tested concentration (50 nM, *in color*) and the calculated theoretical fit (*stippled line*) to a Langmuir interaction. *b*, EphA3-HEK293 cells cultured on fibronectin-coated glass slides were exposed to preclustered, w/t, and mutant ephrin-A5-Fc for 10 min. Cell-morphological and actin-cytoskeletal responses of fixed rhodamine/phalloidin-stained cells were monitored by confocal microscopy. *Scale bar* = 20 μm. *c*, adhesion of cells exposed to preclustered w/t ephrin-A5-Fc or mutants, as indicated, was determined from the area covered by cells in a minimum of three microscopic fields (selected by a blinded observer). Mean and standard deviation from a minimum of three independent experiments is shown. *d*, in parallel experiments, cells were exposed to w/t or mutant ephrin-Fc, equal portions of cell lysates subjected to IPs with anti-EphA3 or anti-CrkII antibodies and probed with anti-EphA3 and anti-phosphotyrosine antibodies as indicated under "Materials and Methods." The immunoblots (*W*/*B*) from three independent experiments were scanned, and relative intensities (mean and S.D.) of individual bands are illustrated together with representative examples of the immunoblots. To assess even gel loading, a sample of the anti-EphA3 IPs was probed with anti-EphA3 antibodies as indicated in the *bottom panel*.

gether with the nearby B–C loop constitutes an additional (third) Eph/ephrin interface (Fig. 1*b*, green) that was not apparent in the crystal structures of the complex of their minimal interaction domains.

Reduced EphA3 Binding Affinities Affect Ephrin-A5-induced Biological Responses—We evaluated whether the reduced binding affinities of the ephrin-A5 mutants cause corresponding effects on EphA3 signaling and downstream cell-morphological responses by assaying typical ephrin-A5-triggered responses, including cell rounding and detachment (Fig. 2 *b*, *c*), as well as EphA3 phosphorylation and recruitment of CrkII (Fig. 2*d*). Purified w/t or mutant ephrin-A5-Fc fusion proteins were used for these experiments, and their binding avidities to EphA3 were confirmed by plasmon resonance analysis (Table II).

As described previously (24), exposure of stably EphA3-transfected HEK293 (EphA3/HEK293) cells to preclustered ephrin-A5-Fc results in dose-dependent cell rounding (Fig. 2*b*) and detachment (Fig. 2*c*). By contrast, treatment of parallel cultures of EphA3/HEK293 cells with the most severely affected mutant, $Thr^{122} \rightarrow Ala$, changed neither the cell morphology nor cell adhesion, as compared with untreated control cells. In agreement, CrkII recruitment was not noticeable in these cells. Interestingly, EphA3 phosphorylation was only reduced but not ablated, in agreement with previous findings that EphA3 phosphorylation and Crk recruitment are not necessarily linked (24). Similarly, exposure of cells to ephrin-A5-Fc mutated in the tetramerization interface ($Asn^{37} \rightarrow Ile$) or the H β-strand ($Phe^{137} \rightarrow Ser$) only weakly modulated cell morphology and cell adhesion. CrkII recruitment and EphA3 phosphorylation were affected for both mutants to similar degrees, suggesting a possible role also of the third ephrin interface for the overall stability of the Eph/ephrin signaling complex. Together, these findings confirm the functional importance of the heterodimerization and the heterotetramerization interfaces for EphA3 binding and activation by ephrin-A5 and, in addition, suggest the essential involvement of a third previously unidentified Eph/ephrin contact site.

DISCUSSION

A unique feature of Eph signaling is the assembly of oligomeric signaling complexes (18, 21), which are required to translate cell surface densities of cognate ephrins into graded cell-morphological responses of Eph-expressing cells (2, 3). Crystallographic analysis of the Eph and ephrin interaction domains unraveled a heterotetrameric complex as an essential building block (8) but also suggested that additional molecular contacts, not apparent in the crystal structures, must be formed to assemble functional signaling clusters.

Here we have identified a cluster of 10 ephrin-A5 residues that are part of the E α-helix and E–F loop, the underlying H β-strand, as well as the nearby B–C loop. Together they form a rugged, convex surface between the heterodimerization and the heterotetramerization domains, providing a third EphA3 interaction site that seems essential for EphA3 signal initiation. In our study, we exploited a library screening approach, designed previously to assign the molecular determinants of EphA3 required for high affinity ephrin binding and formation of functional signaling complexes (17). The strategy is based on the design of a library of mutations randomly distributed across the target sequence, providing an unbiased mutational coverage of the target protein. We argue that, in combination with antibody and protein binding assays as functional read-outs for secreted and (by inference) correctly folded mutant proteins with binding defects for the interaction partner, this approach ensures identification of all relevant interaction sites. Indeed, repeated amino acid substitutions of the same residue through-

TABLE II
Kinetic EphA3-binding characteristics of ephrin-A5 mutants

Protein[a]	Ephrin-A5 dissociation rate[b]	Ephrin-A5 association rate[b]	Ephrin-A5 dissociation constant[b]	Ephrin-A5Fc dissociation constant[c]
	k_d (1/s)	k_a ($1/M\ s^{-1}$)	K_D (M)	K_D (M)
Wild-type ephrin-A5	0.014	1.1×10^6	1.3×10^{-8}	1.7×10^{-11}
Asn^{37}→Ile ephrin-A5	0.003	2.8×10^4	1.22×10^{-7}	3.8×10^{-10}
Gly^{96}→Arg ephrin-A5	0.021	5.1×10^5	4.1×10^{-8}	Not done
Lys^{98}→Asn ephrin-A5	0.022	3.7×10^5	6.0×10^{-8}	1.0×10^{-10}
Thr^{122}→Ala ephrin-A5	0.053	1.8×10^4	2.97×10^{-6}	5.3×10^{-10}
Phe^{137}→Ser ephrin-A5	0.019	4.7×10^5	4.2×10^{-8}	4.0×10^{-11}
Ile^{139}→Thr ephrin-A5	0.024	5.4×10^5	4.5×10^{-8}	Not done

[a] Amino acid changes, as indicated, were introduced into a modified pIg-Bos ephrin-A5-Fc expression vector containing a TEV cleavage site, as described under "Materials and Methods." Mutated ephrin-A5-Fc fusion proteins, harvested from HEK293 supernatants on protein-A-Sepharose, were TEV-cleaved and prepared for BIAcore analysis, as indicated in the legend to Fig. 2*a*.
[b] Kinetic properties, including rate and equilibrium constants, were estimated from BIAcore raw data (seven serial dilutions, 50–0.78 nM, for each protein) using BIAevaluation software (version 3.1) as described previously (17).
[c] Parallel BIAcore experiments were carried out with intact ephrin-A5-Fc and corresponding mutants to estimate relative affinities (avidities) for the divalent (dimeric) proteins.

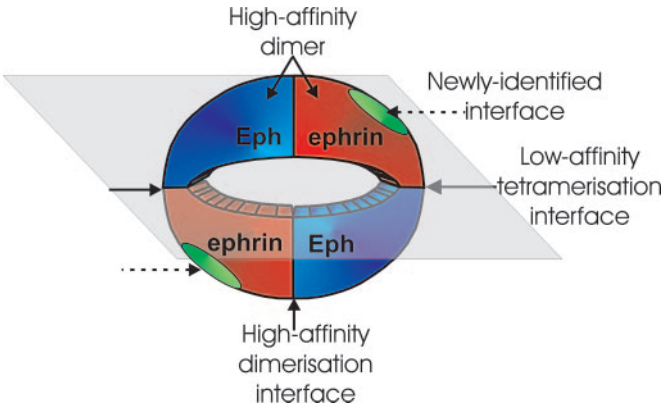

FIG. 3. **Model of the heterotetrameric complex of the minimal Eph/ephrin binding domains.** Two high affinity dimers assemble into a heterotetramer. The localizations of heterodimerization, heterotetramerization, and of the newly identified third interaction surface are indicated.

out the target sequence (Fig. 1*a*) indicate that representative mutants across the complete ephrin-A5 sequence were identified. Our results reveal that, in addition to the known high and low affinity heterodimerization and tetramerization sites, an additional Eph/ephrin interface may be required for receptor activation. Specifically, we postulate that the ephrin-A5 surface (Fig. 1*b*, *green*), located between the previously identified heterodimerization (Fig. 1*b*, *purple*) and tetramerization (Fig. 1*b*, *yellow*) sites, interacts with the cysteine-rich linker of EphA3 (17) to facilitate assembly of tetrameric complexes (Fig. 3) into higher order signaling aggregates. Overall, 30 of the 33 amino acid positions (91%) with function-diminishing mutations are located to these three proposed EphA3 contact sites.

It is interesting that the conserved "YFYIS" motif of the H-strand, which contains 5 of the 10 mutations defining the newly identified Eph-interaction region, is largely buried and mediates packing of the surface E helix and E–F loop against the β-barrel scaffold (14). Thus, it is likely that EphA3 does not interact directly with the ephrin-A5 H-strand but rather with the E helix, the E–F loop, and the B–C loop, which harbor another five receptor mutations. A likely explanation for the fact that we identified a disproportional number of mutations in the H-strand is that single amino acid substitutions there affect the architecture of the whole overlying E helix and E–F loop, thus providing disproportionately large alterations of the local molecular surface. Although we believe that the H-strand mutations will not affect the heterodimerization and heterotetramerization interfaces, we cannot completely rule out this possibility in the absence of detailed structural data. However, we are confident that these mutations do not affect the overall folding and stability of ephrin-A5 as they yield biochemically well behaved proteins that still maintain, to a significant degree, their receptor recognition properties.

Importantly, the assignment of seven function-affecting ephrin-A5 mutations to positions corresponding to the heterotetramerization interface of ephrin-B2 (Fig. 3) verifies that the high affinity ephrin-A5·EphA3 complex has the same heterotetrameric architecture as the structurally elucidated EphB2·ephrin-B2 complex. In agreement with this conclusion, the reduction in EphA3 binding affinity and biological activity observed for the heterotetramerization surface substitution, $Asn^{37} \rightarrow$ Ile (~9-fold reduced affinity, reduced EphA3 activation), and the dimerization surface substitution, $Thr^{122} \rightarrow$ Ala (~50-fold reduced affinity, loss of EphA3 activation), match the effects that would be expected for mutations of these low and high affinity binding sites, respectively. In this context, it is interesting to note that, despite only moderate effects on binding affinity, mutations in the newly identified (third) interaction site substantially reduce the capacity of ephrin-A5 to trigger EphA3 phosphorylation, Crk recruitment, and cell rounding.

We propose that the structural role of the newly identified interaction surface in ephrins is to bind the cysteine-rich domain of an Eph receptor from an adjacent Eph/ephrin tetramer (Fig. 3), thus assembling higher order signaling clusters. The fairly mild effect of the analyzed mutations on EphA3 binding suggests that engagement of this interface, similar to the tetramerization interface, relies on pre-existing, high affinity Eph/ephrin contacts. We speculate that the additional contact through the third interface triggers an EphA3 conformation that favors Eph/Eph oligomerization. It should be noted that it is also possible to model an Eph·ephrin tetrameric complex where all three contact sites are contained within the four interacting Eph and ephrin molecules. In this case, formation of higher order clusters would rely solely on Eph-Eph interactions, a notion supported by the finding that Eph receptors lacking the whole ephrin binding domain are effectively recruited into Eph signaling clusters (25). Thus, a detailed understanding of the precise molecular architecture of the functional Eph/ephrin signaling clusters requires crystallographic analysis of a complex between their complete extracellular domains.

REFERENCES

1. Poliakov, A., Cotrina, M., and Wilkinson, D. G. (2004) *Dev. Cell* 7, 465–480
2. Kullander, K., and Klein, R. (2002) *Nat. Rev. Mol. Cell Biol.* **3,** 475–486
3. Reber, M., Burrola, P., and Lemke, G. (2004) *Nature* **431,** 847–853
4. Mellitzer, G., Xu, Q., and Wilkinson, D. G. (2000) *Curr. Opin. Neuro. Biol.* **10,**

400–408
5. Boyd, A. W., and Lackmann, M. (2001) *Science's STKE*, http://stke.sciencemag.org/cgi/content/full/o_c_sigtrans;2001/112/re20
6. Labrador, J. P., Brambilla, R., and Klein, R. (1997) *EMBO J.* **16,** 3889–3897
7. Lackmann, M., Oates, A. C., Dottori, M., Smith, F. M., Do, C., Power, M., Kravets, L., and Boyd, A. W. (1998) *J. Biol. Chem.* **273,** 20228–20237
8. Himanen, J. P., Rajashankar, K. R., Lackmann, M., Cowan, C. A., Henkemeyer, M., and Nikolov, D. B. (2001) *Nature* **414,** 933–938
9. Himanen, J. P., Henkemeyer, M., and Nikolov, D. B. (1998) *Nature* **396,** 486–491
10. Wybenga-Groot, L. E., Baskin, B., Ong, S. H., Tong, J., Pawson, T., and Sicheri, F. (2001) *Cell* **106,** 745–757
11. Himanen, J. P., and Nikolov, D. B. (2003) *Trends Neurosci.* **26,** 46–51
12. Eph Nomenclature Committee letter (1997) *Cell* **90,** 403–404
13. Gale, N. W., Holland, S. J., Valenzuela, D. M., Flenniken, A., Pan, L., Ryan, T. E., Henkemeyer, M., Strebhardt, K., Hirai, H., Wilkinson, D. G., Pawson, T., Davis, S., and Yancopoulos, G. D. (1996) *Neuron* **17,** 9–19
14. Himanen, J. P., Chumley, M. J., Lackmann, M., Li, C., Barton, W. A., Jeffrey, P. D., Vearing, C., Geleick, D., Feldheim, D. A., Boyd, A. W., Henkemeyer, M., and Nikolov, D. B. (2004) *Nat. Neurosci.* **7,** 501–509
15. Toth, J., Cutforth, T., Gelinas, A. D., Bethoney, K. A., Bard, J., and Harrison, C. J. (2001) *Dev. Cell* **1,** 83–92
16. Lackmann, M., Mann, R. J., Kravets, L., Smith, F. M., Bucci, T. A., Maxwell, K. F., Howlett, G. J., Olsson, J. E., Bos, T. V., Cerretti, D. P., and Boyd, A. W. (1997) *J. Biol. Chem.* **272,** 16521–16530
17. Smith, F. M., Vearing, C., Lackmann, M., Treutlein, H., Himanen, J., Chen, K., Saul, A., Nikolov, D., and Boyd, A. W. (2004) *J. Biol. Chem.* **279,** 9522–9531
18. Stein, E., Lane, A. A., Cerretti, D. P., Schoecklmann, H. O., Schroff, A. D., Van Etten, R. L., and Daniel, T. O. (1998) *Genes Dev.* **12,** 667–678
19. Davis, S., Gale, N. W., Aldrich, T. H., Maisonpierre, P. C., Lhotak, V., Pawson, T., Goldfarb, M., and Yancopoulos, G. D. (1994) *Science* **266,** 816–819
20. Boyd, A. W., Ward, L. D., Wicks, I. P., Simpson, R. J., Salvaris, E., Wilks, A., Welch, K., Loudovaris, M., Rockman, S., and Busmanis, I. (1992) *J. Biol. Chem.* **267,** 3262–3267
21. Huynh-Do, U., Stein, E., Lane, A. A., Liu, H., Cerretti, D. P., and Daniel, T. O. (1999) *EMBO J.* **18,** 2165–2173
22. Lackmann, M., Bucci, T., Mann, R. J., Kravets, L. A., Viney, E., Smith, F., Moritz, R. L., Carter, W., Simpson, R. J., Nicola, N. A., Mackwell, K., Nice, E. C., Wilks, A. F., and Boyd, A. W. (1996) *Proc. Natl. Acad. Sci. U. S. A.* **93,** 2523–2527
23. Jenkins, B. J., D'Andrea, R., and Gonda, T. J. (1995) *EMBO J.* **14,** 4276–4287
24. Lawrenson, I. D., Wimmer-Kleikamp, S. H., Lock, P., Schoenwaelder, S. M., Down, M., Boyd, A. W., Alewood, P. F., and Lackmann, M. (2002) *J. Cell Sci.* **115,** 1059–1072
25. Wimmer-Kleikamp, S. H., Janes, P. W., Squire, A., Bastiaens, P. I., and Lackmann, M. (2004) *J. Cell Biol.* **164,** 661–666
26. Flanagan, J. G., and Vanderhaeghen, P. (1998) *Annu. Rev. Neurosci.* **21,** 309–345

Supplemental data, Table 1. Analysis of surface accessible areas of ephin-A5 residues

VAL	28	136.00	ALA	29	80.00	ASP	30	97.00
ARG	31	99.00	TYR	32	33.00	ALA	33	49.00
VAL	34	1.00	TYR	35	115.00	TRP	36	1.00
ASN	37	34.00	SER	38	50.00	SER	39	101.00
ASN	40	24.00	PRO	41	84.00	ARG	42	114.00
PHE	43	4.00	GLN	44	129.00	ARG	45	172.00
GLY	46	36.00	ASP	47	65.00	TYR	48	9.00
HIS	49	107.00	ILE	50	10.00	ASP	51	62.00
VAL	52	0.00	CYS	53	28.00	ILE	54	37.00
ASN	55	80.00	ASP	56	5.00	TYR	57	68.00
LEU	58	0.00	ASP	59	10.00	VAL	60	0.00
PHE	61	39.00	CYS	62	8.00	PRO	63	3.00
HIS	64	68.00	TYR	65	51.00	GLU	66	136.00
ASP	67	140.00	SER	68	93.00	VAL	69	39.00
PRO	70	60.00	GLU	71	153.00	ASP	72	146.00
LYS	73	152.00	THR	74	11.00	GLU	75	33.00
ARG	76	63.00	TYR	77	21.00	VAL	78	21.00
LEU	79	0.00	TYR	80	34.00	MET	81	9.00
VAL	82	14.00	ASN	83	69.00	PHE	84	99.00
ASP	85	115.00	GLY	86	8.00	TYR	87	14.00
SER	88	62.00	ALA	89	70.00	CYS	90	25.00
ASP	91	39.00	HIS	92	67.00	THR	93	115.00
SER	94	92.00	LYS	95	141.00	GLY	96	47.00
PHE	97	104.00	LYS	98	108.00	ARG	99	40.00
TRP	100	16.00	GLU	101	76.00	CYS	102	2.00
ASN	103	52.00	ARG	104	132.00	PRO	105	16.00
HIS	106	75.00	SER	107	11.00	PRO	108	128.00
ASN	109	152.00	GLY	110	25.00	PRO	111	43.00
LEU	112	43.00	LYS	113	99.00	PHE	114	42.00
SER	115	52.00	GLU	116	6.00	LYS	117	51.00
PHE	118	0.00	GLN	119	44.00	LEU	120	105.00
PHE	121	138.00	THR	122	18.00	PRO	123	95.00
PHE	124	149.00	SER	125	111.00	LEU	126	173.00
GLY	127	38.00	PHE	128	55.00	GLU	129	82.00
PHE	130	3.00	ARG	131	144.00	PRO	132	33.00
GLY	133	41.00	ARG	134	104.00	GLU	135	101.00
TYR	136	25.00	PHE	137	18.00	TYR	138	1.00
ILE	139	0.00	SER	140	4.00	SER	141	18.00
ALA	142	30.00	ILE	143	53.00	PRO	144	59.00
ASP	145	76.00	ASN	146	100.00	GLY	147	71.00
ARG	148	181.00	ARG	149	202.00	SER	150	96.00
CYS	151	31.00	LEU	152	18.00	LYS	153	26.00
LEU	154	1.00	LYS	155	64.00	VAL	156	0.00
PHE	157	64.00	VAL	158	0.00	ARG	159	68.00
PRO	160	43.00	THR	161	105.00	ASN	162	114.00
SER	163	64.00	CYS	164	42.00	MET	165	239.00

Supplementary Table 1. The surface accessible areas (in $Å^2$) of all ephrin-A5 residues present in the crystal structure, PDBID: 1SHX were calculated with the program CCP4 (Collaborative Computational Project, The CCP4 suite: programs for X-ray crystallography. *Acta Crystallogr. D* 50, pp. 760-763, 1994), and are listed together with the sequence position.

Three Distinct Molecular Surfaces in Ephrin-A5 Are Essential for a Functional Interaction with EphA3

Bryan Day, Catherine To, Juha-Pekka Himanen, Fiona M. Smith, Dimitar B. Nikolov, Andrew W. Boyd and Martin Lackmann

J. Biol. Chem. 2005, 280:26526-26532.
doi: 10.1074/jbc.M504972200 originally published online May 18, 2005